

monitor in a region dominated by the CT emission. Thus, we assign the 4–8- μ s component to a predominately MLCT emission while the longer lived component is largely $^3(\pi-\pi^*)$ in character.

The observed $\pi-\pi^*$ phosphorescence τ 's are quite short compared to the millisecond τ 's observed for the purer $^3(\pi-\pi^*)$ phosphorescences for RhL_3^{3+} species.¹⁷ The shortness of our ligand decays arise from spin-orbit coupling mixing the ligand $^3(\pi-\pi^*)$ with allowed states such as the MLCT states.⁴⁶ Mixing will introduce more singlet character into the ligand triplet state, make the ligand phosphorescence more allowed, and shorten its lifetime.

The increase in f_i and K_i/K_s with increasing n confirms the steady-state emission results and shows that increasing n increases the $\pi-\pi^*$ phosphorescence. This is consistent with our interpretation that the fraction of closed form conformers increases with n .

We turn now to a comparison of the room-temperature and 77 K models of Figures 10 and 11. In both cases for long chains some of the conformers invert the ordering of the MLCT and $\pi-\pi^*$ states. The differences in emission parentage arise from the fact that at room temperature the initially excited CT state can lose substantial amounts of energy by solvent reorganization around the new dipole formed in the excited state. This leads to the effective collapse of the band (Figure 11) to a single thermally equilibrated (thexi) state that is the lowest excited state in the molecule. In room-temperature fluid media, this reorganization can occur in a time scale short compared to τ . Thus, excitation of a conformation that would initially have the ^3CT state higher than the $^3(\pi-\pi^*)$ state will promptly relax to a state where the ^3CT state is lower and from which the emission will arise.

In rigid glasses, however, the relaxation time is long compared to τ , and the CT states cannot relax rapidly. Under these conditions, if the excited conformer has the ^3CT state above the $^3(\pi-\pi^*)$ state, this ordering will persist and ligand-localized emission will dominate.

(46) We can exclude shortening of the τ by either kinetic interconversion to the more allowed MLCT state or shortening of lifetime by a low-emission yield. In both cases the Φ_{em} 's would have to be quite low to explain the data, but the yields are much too high. The already high 298 K Φ_{em} 's are increased substantially on cooling to 77 K.

Conclusions

We report a unique intramolecular perturbation of an excited-state manifold by a normally passive alkyl chain. Intramolecular fold back, a strong function of chain length, alters the solvent environment around the excited portion of the molecule with a concomitant change in the state energies and decay paths. Our results suggest that the alkyl chain can function as a molecular switch and invert the lowest excited states in the molecules at low temperature. We suggest that the close proximity of the CT and ligand-localized states of these complexes coupled with the high sensitivity of the CT state energy to its microenvironment accounts to a considerable degree for the large inter- and intramolecular effects observed. The very high environmental sensitivity of these molecules and the ease of making structural modifications suggest their application as site-selective probes of local microstructure in organized media and in biological macromolecules. Further work is in progress.

Acknowledgment. We gratefully acknowledge support by the National Science Foundation (Grant CHE 86-00012) and the American Cancer Society (Grant IN-149B). All lifetime measurements were carried out at the University of Virginia laser facility in part with National Science Foundation Grant CHE 77-09296. We also gratefully acknowledge Hewlett-Packard for the gift of the 8450A spectrophotometer and Henry Wilson for his kind assistance.

Registry No. α -CD, 10016-20-3; β -CD, 7585-39-9; $(\text{bpy})\text{Re}(\text{CO})_3\text{Cl}$, 55658-96-3; $[(\text{bpy})\text{Re}(\text{CO})_3\text{NCCH}_3]^+$, 62972-14-9; $[(\text{bpy})\text{Re}(\text{CO})_3\text{NC}(\text{CH}_2)_2\text{CH}_3](\text{ClO}_4)$, 114597-22-7; $[(\text{bpy})\text{Re}(\text{CO})_3\text{NC}(\text{CH}_2)_5\text{CH}_3](\text{ClO}_4)$, 114614-26-5; $[(\text{bpy})\text{Re}(\text{CO})_3\text{NC}(\text{CH}_2)_7\text{CH}_3](\text{ClO}_4)$, 114597-23-8; $[(\text{bpy})\text{Re}(\text{CO})_3\text{NC}(\text{CH}_2)_9\text{CH}_3](\text{ClO}_4)$, 114597-24-9; $[(\text{bpy})\text{Re}(\text{CO})_3\text{NC}(\text{CH}_2)_{10}\text{CH}_3](\text{ClO}_4)$, 114597-25-0; $[(\text{bpy})\text{Re}(\text{CO})_3\text{NC}(\text{CH}_2)_{13}\text{CH}_3](\text{ClO}_4)$, 114614-27-6; $[(\text{bpy})\text{Re}(\text{CO})_3\text{NC}(\text{CH}_2)_{17}\text{CH}_3](\text{ClO}_4)$, 114597-26-1; O_2 , 7782-44-7.

Supplementary Material Available: Preparation of $[(\text{bpy})\text{Re}(\text{CO})_3\text{NC}(\text{CH}_2)_n\text{CH}_3](\text{ClO}_4)$ and tables of elemental analytical data, electronic UV-visible absorption data, solvent sensitivity, emission spectral data, solvent dependence, excited-state lifetimes, and oxygen-quenching rates (8 pages). Ordering information is given on any current masthead page.

Reactions of Polypyridylchromium(II) Ions with Oxygen: Determination of the Self-Exchange Rate Constant of O_2/O_2^-

Khurram Zahir, James H. Espenson,* and Andreja Bakac*

Contribution from the Ames Laboratory and Department of Chemistry, Iowa State University, Ames, Iowa 50011. Received December 17, 1987

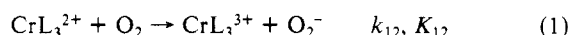
Abstract: Reductive quenching of the ^2E excited states of CrL_3^{3+} complexes, where L is 2,2'-bipyridine (bpy), 1,10-phenanthroline (phen), and their substituted analogues, by disodium ethylenediaminetetraacetate and sodium oxalate was studied by use of laser flash photolysis. The quenching by both compounds results in the rapid, irreversible formation of CrL_3^{2+} with a quantum yield that can approach a value of 2.0. This novel method for the generation of CrL_3^{2+} was utilized to study the reactions of CrL_3^{2+} with ground-state dioxygen. The rate constants for these reactions show a linear dependence on ΔG° as predicted by Marcus theory and range from $2.5 \times 10^5 \text{ M}^{-1} \text{ s}^{-1}$ ($\text{Cr}(\text{5-Clphen})_3^{2+}$) to $2.5 \times 10^7 \text{ M}^{-1} \text{ s}^{-1}$ ($\text{Cr}(\text{Me}_2\text{phen})_3^{2+}$). It is postulated that the reactions proceed by outer-sphere electron transfer to yield superoxide ion as the initial product, as supported by the quantity of H_2O_2 determined after its disproportionation. The electrostatically corrected Marcus cross-relation yielded $k_{22} = 2 \pm 1 \text{ M}^{-1} \text{ s}^{-1}$ for the self-exchange rate constant of the O_2/O_2^- couple. A close inspection of the data obtained in this work along with the literature data strongly suggests that the true value of k_{22} lies in the range $1\text{--}10 \text{ M}^{-1} \text{ s}^{-1}$.

Since the discovery of superoxide dismutase by McCord and Fridovich¹ in 1968, there has been a great deal of interest in the

chemistry of superoxide.^{2–5} One such area of interest relates to the electron-transfer reactions of dioxygen and superoxide with

metal complexes.⁵⁻¹¹ An important parameter that governs those electron-transfer reactions is the rate constant for the O_2/O_2^- self-exchange reaction. To our knowledge, there has been no direct measurement of this intrinsic reactivity parameter, but there have been many attempts to estimate it by use of the Marcus cross-relation.¹¹ Unfortunately, such attempts have led to values that are widely divergent (10^{-8} – 10^7 $M^{-1} s^{-1}$), and the true value of the O_2/O_2^- exchange rate remains to be determined. It is also important to learn whether the wide range of values obtained reflects the inapplicability of Marcus–Hush theory to systems involving small molecules (e.g., O_2/O_2^-), where the reduced and oxidized forms differ greatly from each other in size, charge, and the extent of solvation, or whether some of the systems reported were not simple adiabatic outer-sphere electron-transfer reactions.¹¹

This paper reports our results on the kinetics of the reactions of CrL_3^{2+} with O_2 ($L = 2,2'$ -bipyridine, 1,10-phenanthroline, and their substituted analogues; eq 1). The analysis of the data



according to the Marcus cross-relation equation is warranted by the fact that these reactions occur by an outer-sphere mechanism and have a small or moderate free energy change, such that all the rate constants measured lie well below the diffusion-controlled limit. The kinetic and thermodynamic parameters needed in the treatment were available in the literature.¹²

Experimental Section

Tris(polypyridine)chromium(III) complexes were prepared according to the published procedure,¹³ and the purity was checked by comparison with the reported UV–visible and emission spectra. The emission lifetimes of $*CrL_3^{3+}$ in 1 M HCl agreed well with the literature values.^{12,13} Sodium oxalate (J. T. Baker), disodium ethylenediaminetetraacetate, Na_2H_2edta (Fischer), ferrous ammonium sulfate (99.9%, Aldrich), and $C(NO_2)_4$ (Aldrich) were used as received. Various concentrations of dioxygen in solution were achieved by saturating aqueous solutions by either pure dioxygen or mixtures of N_2/O_2 (Union Carbide).

The kinetic data were obtained by use of the laser flash photolysis system described earlier.¹⁴ The excitation of CrL_3^{3+} complexes was carried out at either 423 or 452 nm by a 600-ns pulse from a Model DL-1100 Phase-R dye laser.

The quenching of $*CrL_3^{3+}$ by $C_2O_4^{2-}$ and H_2edta^{2-} was monitored at the emission maximum of $*CrL_3^{3+}$ at 730 nm. The quantum yield measurements for the formation of CrL_3^{2+} were carried out with both quenchers for $L = bpy$. The concentration of $*Cr(bpy)_3^{3+}$ in these

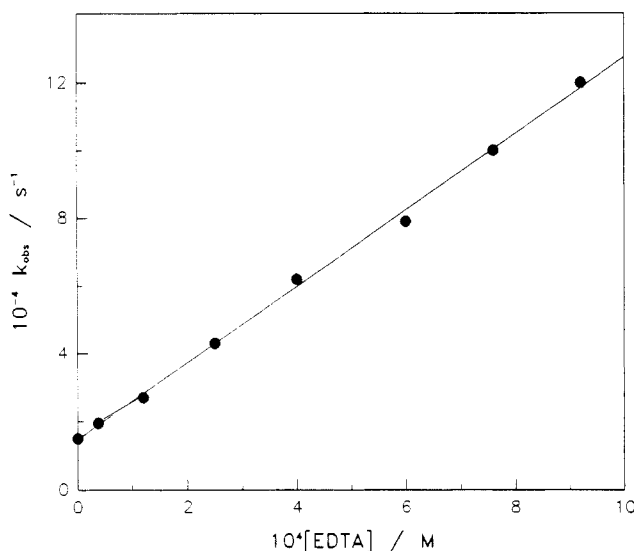


Figure 1. Plot of the observed rate constant for the quenching of $*Cr(bpy)_3^{3+}$ by H_2edta^{2-} versus the concentration of H_2edta^{2-} at ambient temperature and 0.05 M ionic strength (Na_2SO_4).

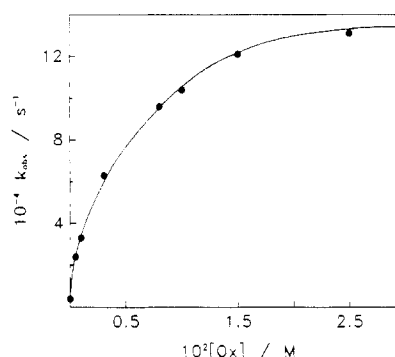


Figure 2. Plot of the observed rate constant for the quenching of $*Cr(phen)_3^{3+}$ by $Na_2C_2O_4$ versus the concentration of $Na_2C_2O_4$ at ambient temperature. No adjustment of the ionic strength was made.

experiments was determined from the absorbance changes at λ 445 nm in the absence of quenchers. The yield of the $Cr(bpy)_3^{2+}$, obtained in the quenching reaction, was calculated from the absorbance changes at 560 and 470 nm. The formation and/or decay of other CrL_3^{2+} complexes was monitored at 440 nm ($L = 5$ -Clphen), 560 and 470 (Me_2bpy), 430 (phen), 480 and 685 (5 -Mephen), and 430 (Me_2phen).^{12,13,15}

The reactions between CrL_3^{2+} and O_2 were studied by monitoring the disappearance of CrL_3^{2+} (typically 8–12 μM) in the presence of a pseudo-first-order excess of dioxygen. The rate constants were obtained by the nonlinear least-squares analysis of the exponential absorbance–time curves.

Hydrogen peroxide was identified and determined in product solutions from the rate and extent of the absorbance increase at 353 nm corresponding to the formation of I_3^- (ϵ 2.6×10^4 $M^{-1} cm^{-1}$) in H_2SO_4 solutions. Control experiments consisted of using solutions in which the same reagents were present but that had not received any laser pulses. Hydrogen peroxide was found to be completely absent from the controls. Subsequent addition of authentic H_2O_2 to the control gave the same absorbance change as in the actual experiment, and that change occurred with the same rate as in the sample itself.

Results

Quenching of $*CrL_3^{3+}$ by Na_2H_2edta and $Na_2C_2O_4$. Figures 1 and 2 show the plots of the reciprocal of the lifetime (k_{obsd}) as a function of the quencher concentration for the quenching of $*Cr(bpy)_3^{3+}$ by H_2edta^{2-} and $*Cr(phen)_3^{3+}$ by $C_2O_4^{2-}$, respectively. As shown in Figure 1, k_{obsd} increases linearly with increasing $[H_2edta^{2-}]$, giving a value of $k_q = 1.2 (\pm 0.2) \times 10^8$ $M^{-1} s^{-1}$ for

- (1) (a) McCord, J. M.; Fridovich, I. *J. Biol. Chem.* **1968**, *243*, 5757. (b) *Ibid.* **1969**, *244*, 6049.
- (2) Michaelson, A. M.; McCord, J. M.; Fridovich, I. *Superoxide and Superoxide Dismutase*; Academic: New York, 1977.
- (3) (a) Sawyer, D. T.; Valentine, J. C. *Acc. Chem. Res.* **1981**, *14*, 393. (b) Valentine, J. C. In *Biochemical and Clinical Aspects of Oxygen*; Caughey, C. W., Ed.; Academic: New York, 1979; pp 657–677.
- (4) Fee, A. J. In *Oxygen and Oxy Radicals in Chemistry and Biology*; Rodger, M. A. J.; Powers, E. L., Eds.; Academic: New York, 1981; pp 206.
- (5) Sawyer, D. T.; Nanni, E. J., Jr.; Roberts, J. L., Jr. In *Electrochemical and Spectroelectrochemical Studies of Biological Redox Compounds*; Kadish, K., Ed.; American Chemical Society: Washington, DC, 1982; pp 585–600.
- (6) Bielski, B. H. J.; Cabelli, D. E.; Arudi, R. L.; Ross, A. B. *J. Phys. Chem. Ref. Data* **1985**, *14*, 1041.
- (7) Pladziewicz, J. R.; Meyer, T. J.; Broomhead, J. A.; Taube, H. *Inorg. Chem.* **1980**, *19*, 3735.
- (8) Stanbury, D. M.; Haas, O.; Taube, H. *Inorg. Chem.* **1980**, *19*, 518.
- (9) Stanbury, D. M.; Mulac, W. A.; Sullivan, J. C.; Taube, H. *Inorg. Chem.* **1980**, *19*, 3735.
- (10) Stanbury, D. M.; Gaswick, D.; Brown, G. M.; Taube, H. *Inorg. Chem.* **1983**, *22*, 1975.
- (11) Bakac, A.; Espenson, J. H.; Creaser, I. I.; Sargeson, A. M. *J. Am. Chem. Soc.* **1983**, *105*, 7624.
- (12) Creaser, I. I.; Geue, R. J.; Harrowfield, J. MacB.; Herlt, A. J.; Sargeson, A. M.; Snow, M. R.; Springborg, J. *J. Am. Chem. Soc.* **1982**, *104*, 6016.
- (13) McDowell, S. M.; Espenson, J. H.; Bakac, A. *Inorg. Chem.* **1984**, *23*, 2232.
- (14) Jamieson, M. A.; Serpone, N.; Hoffman, M. Z. *Coord. Chem. Rev.* **1981**, *39*, 121.
- (15) Brunschwig, B.; Sutin, N. *J. Am. Chem. Soc.* **1978**, *100*, 7568.
- (16) Melton, J. D.; Espenson, J. H.; Bakac, A. *Inorg. Chem.* **1986**, *25*, 4104.

- (15) (a) Konig, E.; Herzog, S. *J. Inorg. Nucl. Chem.* **1970**, *32*, 585. (b) Serpone, N.; Jamieson, M. A.; Emmi, S. S.; Fouchi, P. G.; Mulazzani, Q. G.; Hoffman, M. Z. *J. Am. Chem. Soc.* **1981**, *103*, 1091.

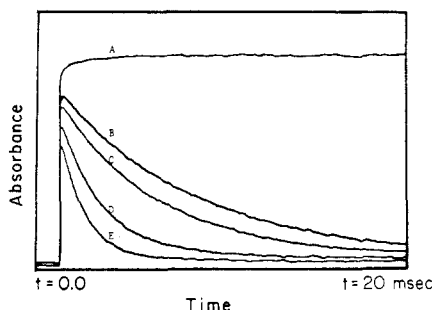
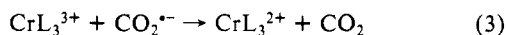
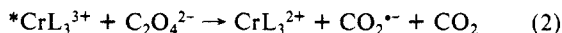


Figure 3. Formation of $\text{Cr}(\text{bpy})_3^{2+}$ by reductive quenching of $^*\text{Cr}(\text{bpy})_3^{3+}$ by $\text{Na}_2\text{C}_2\text{O}_4$ (0.05 M) observed at 560 nm and the disappearance of $\text{Cr}(\text{bpy})_3^{2+}$ in the reaction with dioxygen. The concentrations of oxygen are 0.0 (A), 2.9×10^{-4} (B), 4.0×10^{-4} (C), 8.5×10^{-4} (D), and 1.3×10^{-3} M (E).

the quenching of $^*\text{Cr}(\text{bpy})_3^{3+}$. Similar plots yielded values of $5.2 (\pm 0.5) \times 10^8 \text{ M}^{-1} \text{ s}^{-1}$ for $^*\text{Cr}(\text{5-Clphen})_3^{3+}$ and $7.3 (\pm 0.6) \times 10^7 \text{ M}^{-1} \text{ s}^{-1}$ for $^*\text{Cr}(\text{Me}_2\text{phen})_3^{3+}$. The quenching by $\text{C}_2\text{O}_4^{2-}$ yielded nonlinear plots of k_{obsd} versus $[\text{C}_2\text{O}_4^{2-}]$, as shown in Figure 2 for $\text{Cr}(\text{phen})_3^{3+}$. A detailed account of this phenomenon will be presented elsewhere.¹⁶

Quenching Mechanism and Quantum Yields. The quenching of $^*\text{CrL}_3^{3+}$ by $\text{H}_2\text{edta}^{2-}$ and $\text{C}_2\text{O}_4^{2-}$ yielded CrL_3^{2+} in all the cases examined. A solution containing 11 μM $^*\text{Cr}(\text{bpy})_3^{3+}$, 120 μM $\text{Cr}(\text{bpy})_3^{3+}$, and 0.065 M $\text{Na}_2\text{C}_2\text{O}_4$ yielded 23 μM $\text{Cr}(\text{bpy})_3^{2+}$. In another experiment using 6.2 μM $^*\text{Cr}(\text{bpy})_3^{3+}$, 86 μM $\text{Cr}(\text{bpy})_3^{3+}$, and 0.010 M $\text{Na}_2\text{H}_2\text{edta}$, the concentration of $\text{Cr}(\text{bpy})_3^{2+}$ produced was 13 μM . The quantum yield for the formation of $\text{Cr}(\text{bpy})_3^{2+}$ by reductive quenching of $^*\text{CrL}_3^{3+}$ by $\text{Na}_2\text{C}_2\text{O}_4$ and $\text{Na}_2\text{H}_2\text{edta}$ is thus 2.0 under our experimental conditions. The same quantum yield was assumed, but not verified, for the formation of all the other CrL_3^{2+} complexes.

The dependence of the quenching rate constants on the driving force for the reactions, as well as the formation of CrL_3^{2+} , is consistent with an electron-transfer mechanism (eq 2 and 3).



A similar mechanism is suggested for the quenching by $\text{H}_2\text{edta}^{2-}$. The one-electron-oxidized $\text{H}_2\text{edta}^{2-}$ attacks the ground-state CrL_3^{3+} to yield the second mole of CrL_3^{2+} . The scheme is completed by the decomposition of the products derived from $\text{H}_2\text{edta}^{2-}$.

The rapid and irreversible formation of CrL_3^{2+} in the reductive quenching of $^*\text{CrL}_3^{3+}$ by $\text{H}_2\text{edta}^{2-}$ and $\text{C}_2\text{O}_4^{2-}$ provides us with an easily accessible source of long-lived CrL_3^{2+} . In the absence of any added reagents under air-free conditions no change in $[\text{CrL}_3^{2+}]$ was observed in 50 ms.

In several experiments the CrL_3^{2+} was also generated by use of Fe^{2+} as a quencher for $^*\text{CrL}_3^{3+}$.¹⁷

Kinetics of CrL_3^{2+} - O_2 Reaction. In the presence of oxygen CrL_3^{2+} disappears rapidly, Figure 3, according to eq 4 and 5. The

$$-\text{d}[\text{CrL}_3^{2+}]/\text{d}t = k_{\text{obsd}}[\text{CrL}_3^{2+}] \quad (4)$$

$$k_{\text{obsd}} = k_{12}[\text{O}_2] \quad (5)$$

results were identical irrespective of the quencher used in the preparation of CrL_3^{2+} .

The rate constants k_{obsd} increased linearly with increasing concentration of dioxygen. One particular set of kinetic data is collected in Table I. The plots of k_{obsd} versus $[\text{O}_2]$ for all the complexes are shown in Figure 4. The values of the second-order rate constants were obtained from the slopes of such plots, and the results are presented in Table II.

The quenching of $^*\text{CrL}_3^{3+}$ by O_2 (eq 6) was insignificant most of the time. In several experiments that should have yielded some

Table I. Summary of the Rate Constants ($10^{-3}k_{\text{obsd}}/\text{s}^{-1}$) for the Reduction of O_2 by CrL_3^{2+} Complexes^a

| $10^4[\text{O}_2]/\text{M}$ | L | | | | | |
|-----------------------------|----------|-------|-------|----------|---------------------|----------------------|
| | 5-Clphen | bpy | phen | 5-Mephen | Me ₂ bpy | Me ₂ phen |
| 2.9 | 0.070 | 0.170 | 0.440 | 0.66 | 3.76 | 7.24 |
| 4.0 | 0.10 | 0.230 | 0.610 | 0.88 | 5.60 | 10.5 |
| 6.5 | 0.166 | 0.395 | 0.940 | 1.45 | 9.2 | |
| 8.5 | 0.210 | 0.510 | 1.23 | 1.85 | 12.0 | |
| 13.0 | 0.330 | 0.760 | 1.90 | 2.75 | 17.5 | |

^a In H_2O at $22 \pm 2^\circ\text{C}$, μ 0.15 M, pH 5.8. Solutions were saturated with N_2/O_2 gas mixtures containing varying concentrations of O_2 . $\text{Na}_2\text{C}_2\text{O}_4$ (0.05 M) was used as a quencher.

Table II. Second-Order Rate Constants for the Reduction of Dioxygen^a by CrL_3^{2+} Complexes

| L | ΔE° b/V | $10^{-5}k_{12}/\text{M}^{-1} \text{ s}^{-1}$ |
|--------------------------|----------------------|--|
| 5-Clphen | 0.01 | $2.5 \pm 0.03^{c,d}$ |
| bpy | 0.1 | $6.0 \pm 0.4^{e,f}$ |
| | | $6.1 \pm 0.4^{e,f}$ |
| | | $6.0 \pm 0.4^{e,g}$ |
| | | $6.2 \pm 0.4^{e,f}$ |
| phen | 0.12 | $14 \pm 1^{c,i}$ |
| | | $15.5 \pm 2^{f,i}$ |
| | | $15.6 \pm 2^{g,i}$ |
| | | $15 \pm 2^{c,j}$ |
| 5-Mephen | 0.15 | $22 \pm 2^{c,h}$ |
| 4,4'-Me ₂ bpy | 0.29 | $140 \pm 10^{c,e}$ |
| | | $135 \pm 10^{e,f}$ |
| | | $140 \pm 10^{c,h}$ |
| | | $180 \pm 10^{e,k}$ |
| 4,7-Me ₂ phen | 0.29 | $250 \pm 45^{c,i}$ |
| | | $280 \pm 40^{f,i}$ |

^a $[\text{CrL}_3^{3+}] = (1.0\text{--}1.6) \times 10^{-4} \text{ M}$, unless stated otherwise; $T = 22 \pm 2^\circ\text{C}$. ^b From data in ref 12 and $E^\circ(\text{O}_2/\text{O}_2^{\cdot-}) = -0.16 \text{ V}$. ^c Quenching by 0.050 M oxalate. ^d Monitored at λ 440 nm. ^e λ 560 nm. ^f Quenching by 1.4 mM $\text{H}_2\text{edta}^{2-}$. ^g $[\text{CrL}_3^{3+}] = 3.3 \times 10^{-4} \text{ M}$, $[\text{oxalate}] = 0.1 \text{ M}$. ^h λ 480 nm. ⁱ λ 430 nm. ^j λ 450 or 690 nm. ^k Quenching by 0.010 M Fe^{2+} .

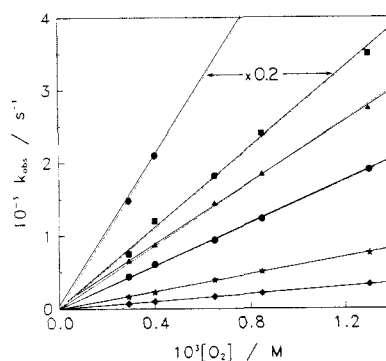
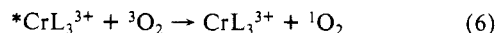


Figure 4. Plot of k_{obsd} , the observed rate constant for the reduction of dioxygen by CrL_3^{2+} complexes, versus $[\text{O}_2]$. The data are shown for L = 5-Clphen (diamonds), bpy (stars), phen (dots), 5-Mephen (triangles), Me_2bpy (squares), and Me_2phen (asterisks). The rate constants for the two fastest reactions were multiplied by 0.2 so they could be displayed on this scale.

$^1\text{O}_2$, owing to the slower quenching by $\text{Na}_2\text{H}_2\text{edta}$ or $\text{Na}_2\text{C}_2\text{O}_4$ at lower concentration, no complications were noted, apparently because the lifetime of $^1\text{O}_2$ is quite short (4 μs) under our experimental conditions.¹⁸



Detection of Superoxide Ion. Experiments were done to detect $\text{O}_2^{\cdot-}$ directly by such standard superoxide indicators as tetranitromethane and nitro blue tetrazolium.⁵ These experiments failed, owing to rapid direct reactions between these reagents and CrL_3^{2+} . In retrospect, this is not too surprising since the trapping reactions are one-electron-transfer reactions and CrL_3^{2+} complexes

(16) Steffan, C.; Espenson, J. H.; Bakac, A., to be submitted for publication.

(17) Bakac, A.; Zahir, K.; Espenson, J. H. *Inorg. Chem.* **1988**, 27, 315.

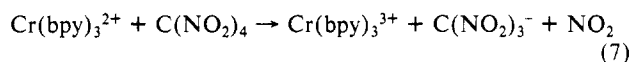
(18) Rodgers, M. A. J. *Photochem. Photobiol.* **1983**, 37, 99.

Table III. Summary of the Data on the Outer-Sphere Oxidations by O₂^a

| reductant | $k_{12}/\text{M}^{-1} \text{ s}^{-1}$ | k_{11}/M^{-1} | $r/\text{\AA}$ | K_{eq} | $k_{22}/\text{M}^{-1} \text{ s}^{-1}$ | ref |
|--|---------------------------------------|--------------------------------|----------------|-----------------------|---------------------------------------|-----|
| Cr(5-Clphen) ₃ ²⁺ | 2.5×10^5 | 1×10^9 ^b | 6.8 | 1.5 | 3.4 | c |
| Cr(bpy) ₃ ²⁺ | 6.0×10^5 | 1×10^9 | 6.8 | 4.9×10 | 0.8 | c |
| Cr(phen) ₃ ²⁺ | 1.5×10^6 | 1×10^9 | 6.8 | 1.06×10^2 | 2.0 | c |
| Cr(5-Mephen) ₃ ²⁺ | 2.2×10^6 | 1×10^9 | 6.8 | 3.45×10^2 | 1.7 | c |
| Cr(4,4'-Me ₂ bpy) ₃ ²⁺ | 1.4×10^7 | 1×10^9 | 6.8 | 8.0×10^4 | 0.8 | c |
| Cr(4,7-Me ₂ phen) ₃ ²⁺ | 2.5×10^7 | 1×10^9 | 6.8 | 8.0×10^4 | 2.5 | c |
| Ru(NH ₃) ₆ ²⁺ | 6.3×10 | 3.0×10^3 ^d | 3.4 | 2.7×10^{-4} | 8.2 | e |
| Ru(NH ₃) ₄ phen ²⁺ | 7.7×10^{-3} | 1.2×10^7 | 4.5 | 2.0×10^{-12} | 1.4 | e |
| Ru(NH ₃) ₅ (isn) ²⁺ | 1.1×10^{-1} | 4.7×10^5 | 4.5 | 5.7×10^{-10} | 5.1 | e |
| Ru(NH ₃) ₅ (4-vinyl-py) ²⁺ | 5.7×10^{-1} | 5.0×10^4 | 4.5 | 1.7×10^{-8} | 7.7 | e |
| Ru(en) ₃ ²⁺ | 3.6×10 | 2.0×10^4 | 4.0 | 2.5×10^{-6} | 260 | e |
| Co(sep) ₃ ²⁺ | 4.3×10 | 5.1 (2.1) ^f | 4.5 | 4.9×10 | 0.6 (1.2) | g |

^a Rate constants at $22 \pm 2^\circ \text{C}$ and μ 0.1 M; bpy = 2,2'-bipyridine, phen = 1,10-phenanthroline, en = ethylenediamine, sep = sepulchrate, py = pyridine, isn = isonicotinamide. The value $r = 1.33 \text{ \AA}$ was used for O₂⁻. ^b Reference 13. ^c This work. ^d μ 0.2 M. ^e Reference 7. ^f Corrected to ionic strength at 0.1 M. ^g Reference 10.

are stronger reducing agents¹² with higher self-exchange rate constants than O₂⁻. Indeed, we can report that the reaction between Cr(bpy)₃²⁺ and C(NO₂)₄ occurs with a clean 1:1 stoichiometry to produce C(NO₂)₃⁻ (λ_{max} 350 nm, ϵ $1.5 \times 10^4 \text{ M}^{-1} \text{ cm}^{-1}$)¹⁹ quantitatively, as in eq 7. A cursory kinetic study gave $k_7 \approx 3 \times 10^9 \text{ M}^{-1} \text{ s}^{-1}$ at pH 7.



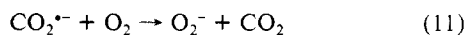
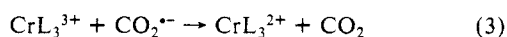
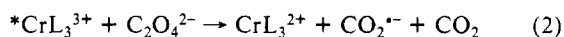
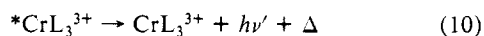
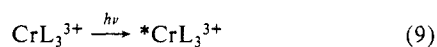
We therefore had to resort to an indirect method to establish that O₂⁻ was the initial reaction product. We relied on the rapid disproportionation reaction ($2\text{O}_2^- + 2\text{H}_2\text{O} \rightarrow \text{H}_2\text{O}_2 + \text{O}_2 + 2\text{OH}^-$) and succeeded in determining the concentration of H₂O₂ produced. An aqueous solution of $2.2 \times 10^{-4} \text{ M}$ Cr(bpy)₃³⁺ and 5 mM Na₂H₂edta was flashed four times with 460-nm laser light. Each flash produced $\sim 2 \times 10^{-5} \text{ M}$ Cr(bpy)₃²⁺ that subsequently reacted with O₂ to regenerate Cr(bpy)₃³⁺. The solution was acidified and shown to contain $4 \times 10^{-5} \text{ M}$ H₂O₂. The stoichiometry of the overall reaction is thus given by eq 8, which is consistent with (but not absolute proof of) a scheme in which O₂⁻ is the immediate product of reaction 1.



Discussion

CrL₃²⁺-O₂ Reactions. The sequence of events that leads to the formation of CrL₃²⁺ and to its subsequent reaction with dioxygen is given in Scheme I and eq 1. In the presence of O₂ the fate of CO₂⁻ is no longer exclusively reduction of CrL₃³⁺ (eq 3). Competing with that is the reduction of O₂ to O₂⁻ by CO₂⁻ (eq 11, $k_{11} = 4.2 \times 10^9 \text{ M}^{-1} \text{ s}^{-1}$).²⁰ This lowers the initial concentration of CrL₃²⁺ (in the limit, to the $\Phi = 1$ value) but is otherwise without effect. On the basis of the yields of CrL₃²⁺ in solutions containing oxygen and the known value of k_{11} , we estimate $k_3 \approx 10^{10} \text{ M}^{-1} \text{ s}^{-1}$. Note the decline in the initial concentration of Cr(bpy)₃²⁺ with increasing [O₂] (Figure 3).

Scheme I



The single most decisive piece of evidence for the one-electron-transfer step of eq 1 would be provided by a direct observation or trapping of O₂⁻. The former is ruled out by the fact that chromium polypyridine complexes absorb much more strongly

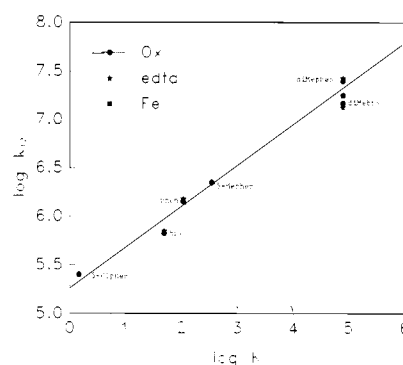
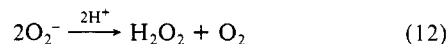


Figure 5. Plot of $\log k_{12}$, the logarithm of the rate constants for the reduction of O₂ by CrL₃²⁺, versus $\log K$, the logarithm of the equilibrium constant for the reactions. Identical results were obtained with all three quenchers used for the production of CrL₃²⁺. The quenchers used were oxalate (circles), Na₂H₂edta (stars), and Fe_{aq}²⁺ (squares).

throughout the UV-visible range than O₂⁻ does. The trapping of O₂⁻ was thwarted by the rapid reactions of CrL₃²⁺ with the superoxide traps. However, there is little doubt that O₂⁻ is indeed involved.

The overall reaction is shown in eq 8. An inner-sphere mechanism for this reaction is highly unlikely, owing to the lack of the available coordination site on CrL₃²⁺.²¹ An attack at the polypyridine ligand is also implausible and without a precedent. An outer-sphere reaction, on the other hand, seems quite likely in view of the known reactivity of both O₂ (Table III) and CrL₃²⁺²² in outer-sphere electron-transfer reactions. The excellent adherence of all the kinetic data in this work to the Marcus-Hush theory, as discussed later, is also taken as a strong evidence for the proposed outer-sphere mechanism.

The superoxide, produced in reaction 1, most likely disproportionates (eq 12). The other possibility that would satisfy the



overall stoichiometry of eq 8 is the oxidation of Cr(bpy)₃²⁺. An outer-sphere oxidation by O₂⁻ is quite unlikely,^{5,23} but we do not have enough experimental evidence to rule out completely a more complicated reaction involving the ligands.

As expected, the values of k_{12} increase with the free energy of the reaction. The Marcus-Hush theory²⁴ predicts the following

(21) The polypyridine complexes of chromium(II) are substitutionally quite inert. The irreversible loss of the ligands in acidic solutions occurs on the time scales that are orders of magnitude longer than those involved in this work.

(22) (a) Candlin, J. P.; Halpern, J.; Trimm, D. L. *J. Am. Chem. Soc.* **1964**, *86*, 1019. (b) Zwickel, A. M.; Taube, H. *Discuss. Faraday Soc.* **1960**, *29*, 42. (c) Beattie, J. K.; Binstead, R. A.; Broccardo, M. *Inorg. Chem.* **1978**, *17*, 1822.

(23) Sawyer, D. T.; Valentine, J. S. *Acc. Chem. Res.* **1981**, *14*, 393.

(24) (a) Marcus, R. A. *J. Chem. Phys.* **1965**, *43*, 679, 2654. (b) Marcus, R. A.; Sutin, N. *Biochem. Biophys. Acta* **1985**, *811*, 265. (c) Hush, N. S. *Trans. Faraday Soc.* **1961**, *57*, 557. (d) Hush, N. S. *Prog. Inorg. Chem.* **1967**, *8*, 391.

(19) (a) Henglein, A.; Jaspert, J. *Neue Folge* **1957**, *12*, 324. (b) Asmus, K.-D.; Möckel, H.; Henglein, A. *J. Phys. Chem.* **1973**, *77*, 1218.

(20) Ilan, Y.; Rabani, J. *Int. J. Radiat. Phys. Chem.* **1976**, *8*, 609.

Table IV. Summary of the Data on the Reductions by O_2^-

| oxidant | k_{-12}^a | k_{11} | $r/\text{\AA}$ | K_{eq} | k_{22} | ref |
|-------------------|-------------------|----------------------|----------------|----------------------|--------------------|-----|
| $Fe(CN)_6^{3-}$ | 3×10^2 | 5×10^3 | 4.5 | 9.6×10^8 | 1×10^{-8} | b |
| $Mo(CN)_8^{3-}$ | 3×10^5 | 3×10^4 | 5.0 | 3×10^{15} | 8×10^{-8} | c |
| $Fe(cp)_2^+$ | 8.6×10^6 | 6×10^6 | 5.0 | 7×10^{11} | 2×10^{-3} | d |
| $Fe(edta)-H_2O^-$ | 2×10^6 | 3×10^4 | 4.5 | 5.4×10^4 | 7.2×10^3 | e |
| $Co(en)_3^{3+}$ | 24 | 2.4×10^{-5} | 4.5 | 4.4×10^{-2} | 4.6×10^5 | f |
| quinones | 10^6-10^8 | 1×10^7 | | $10^{-2}-10^4$ | 10^6-10^7 | g |

^aRate constants ($M^{-1} s^{-1}$) at $22 \pm 2^\circ C$. ^bReference 30. ^cReference 31. ^dReference 11. The value $k_{22} = 6.9 \times 10^{-5} M^{-1} s^{-1}$, reported in ref 11, is erroneous. ^eBull, C.; McClune, G. J.; Fee, J. A. *J. Am. Chem. Soc.* **1983**, *105*, 5290. ^fReference 11. ^gReferences 27 and 28.

relationship between the rate and equilibrium constants for outer-sphere electron-transfer reactions (eq 13). A plot of log

$$k_{12} = (k_{11}k_{22}K_{12}f_{12})^{1/2} \quad (13)$$

$$\log f_{12} = (\log K_{12})^{1/2} / [4 \log (k_{11}k_{22}/Z^2)]$$

k_{12} against K_{12} is shown in Figure 5. The plot is linear and yields a slope of 0.41, in good agreement with the value of 0.5 predicted by the theory.

O_2/O_2^- Self-Exchange Rate. The Marcus cross relation (eq 13) has been previously utilized to evaluate this self-exchange rate constant.^{7,8,11} As these calculations involve redox couples of different charge type, it is necessary to include the work term (eq 14–17) where a is the distance of closest approach and is taken as the sum of the radii of the two reactants, Z is the collision frequency, and the other terms have their usual meaning.²⁴

$$k_{12} = (k_{11}k_{22}K_{12}f_{12})^{1/2}W_{12} \quad (14)$$

$$\ln f_{12} = \frac{[\ln K_{12} + (w_{12} - w_{21})/RT]^2}{4 \ln (k_{11}k_{22}/Z^2) + (w_{11} + w_{22})/RT} \quad (15)$$

$$W_{12} = \exp[-(w_{12} + w_{21} - w_{11} - w_{22})/2RT] \quad (16)$$

$$w_{ij} = \frac{(4.225 \times 10^{-8})Z_iZ_j}{a(1 + (3.285 \times 10^7)a\mu^{1/2})} \quad (17)$$

The present results and those on the related systems for which kinetic and thermodynamic data are available were subjected to such treatment. The values of k_{22} , the self-exchange rate constant for O_2/O_2^- so obtained, are collected in Tables III and IV.^{25,26}

(25) Wilkins and co-workers have studied the reactions of mono- and bisviologens with dioxygen.²⁶ A value of $3.5 \times 10^{13} M^{-2} s^{-2}$ was obtained for the product of self-exchange rate constants for viologens and O_2 from a plot of $\ln k_{12}$ versus $\ln K_{12}/f_{12}$. We are not confident whether the Marcus cross relation should be applied to these systems as some of these viologens are not adequately modeled as spheres. In addition, some specific (strong) interactions between the viologens and O_2/O_2^- may occur, resulting in too high a self-exchange rate.

The reactions of CrL_3^{2+} yielded $k_{22} = 1-4 M^{-1} s^{-1}$. The values derived from all the other autoxidation reactions lie in the range $1-10 M^{-1} s^{-1}$. The only exception is $Ru(en)_3^{2+}$, and even that gives an almost acceptable k_{22} of $260 M^{-1} s^{-1}$. The self-exchange rate constant k_{11} for $Ru(en)_3^{2+/3+}$ was estimated⁷ as being approximately 5 times higher than that for the hexaammine complex, but no measurement has been made.

The large number of data in Table III and the narrow range of k_{22} values are quite encouraging and indicate that Marcus-Hush theory is applicable to outer-sphere autoxidations. A close examination of the data shows that the highly scattered¹¹ values of k_{22} are all derived from the reductions by O_2^- (Table IV).

The data for $Co(en)_3^{3+}$ should probably be excluded, since the rate constant for the reaction of the closely related $Co(sep)^{3+}$ with O_2^- under catalytic conditions gave a value much larger than that calculated⁹ from the measured rate constant for the autoxidation of $Co(sep)^{2+}$ and the equilibrium constant. This result implies that the observed reaction between $Co(sep)^{3+}$ and O_2^- (and by analogy the reaction of $Co(en)_3^{3+}$ with O_2^-) is not the reverse of autoxidation but some other unidentified process. The reduction of the other oxidants in Table IV by O_2^- has been observed directly, thus leaving little doubt that the measured rate constants correspond to the assigned reactions.

Several problems may be associated with the reactions in Table IV. For example, a possibility has been raised that quinones^{27,28} react with O_2^- by a ring addition.⁷ The reaction of $Fe(cp)_2^+$ with O_2^- is apparently nonadiabatic in CH_3CN ,²⁹ and the same might be true in aqueous solutions. The strong ion pairing with the counterions might well influence the kinetics of the reactions of $Fe(CN)_6^{3-30}$ and $Mo(CN)_8^{3-31}$.

While all these possibilities seem quite legitimate, it is still puzzling that all the problematic reactions involve O_2^- and all the reactions with O_2 are in good agreement with each other. This may be a coincidence, but it might also point to some complicated interactions between O_2^- and the oxidants in Table IV.

Acknowledgment. This research was supported by the National Science Foundation, Grant CHE-8418084. Some of the facilities for this work were provided by the Ames Laboratory, which is operated by Iowa State University under Contract W-7405-Eng-82. We are indebted to Dr. N. Sutin for his expert opinion and useful comments.

(26) Atherton, S. J.; Tsukahara, K.; Wilkins, R. G. *J. Am. Chem. Soc.* **1986**, *108*, 3380.

(27) Patel, K. B.; Willson, R. B. *J. Chem. Soc., Faraday Trans 1* **1973**, *69*, 814.

(28) Meisel, D. *Chem. Phys. Lett.* **1975**, *34*, 263.

(29) Zahir, K.; Haim, A., unpublished observations. This conclusion was based on the high yields of 1O_2 in this reaction.

(30) Zehavi, D.; Rabani, J. *J. Phys. Chem.* **1972**, *76*, 3703.

(31) Faraggi, M. J. *J. Phys. Chem.* **1976**, *80*, 2316.